The Flux of Atmospheric Water Vapor over the Caribbean Sea and the Gulf of Mexico

STEFAN L. HASTENRATH

The University of Wisconsin, Madison

(Manuscript received 8 June 1966, in revised form 11 July 1966)

ABSTRACT

The flux of atmospheric water vapor has been examined as part of a more extensive study on general circulation and energetics in the area of the Central American seas. The analysis is based on twice daily radiosonde data for the entire year 1960. During the winter half of the year, a westward directed moisture transport is concentrated in a relatively narrow band over the southern Caribbean Sea. The flux of water vapor over the Gulf of Mexico is directed roughly eastward. An increase of the transport downstream indicates the excess of evaporation over precipitation. In summer, a strong moisture flux extends from the Caribbean Sea over the Gulf of Mexico into the interior of the North American continent. The water vapor transport decreases downstream, which means an excess of precipitation over evaporation. The eddy moisture flux and flux divergence over the Gulf of Mexico reaches considerable proportions in winter, while it is comparatively small over the Caribbean Sea throughout the year. The water vapor flux divergence is discussed with regard to estimates of large-scale precipitation and independent computations of the sensible and latent heat flux at the sea-air interface.

1. Introduction

Increasing attention has been drawn in recent years to the water vapor transfer and the large-scale divergence of the atmospheric moisture flux (e.g., Möller and de Bary, 1951; Benton and Estoque, 1954; Hutchings, 1957). Interest focuses on such aspects as the water vapor transport as a factor in the general circulation (Starr and White, 1955; Sutcliffe, 1956; Starr *et al.*, 1958; Starr and Peixoto, 1960, 1964), its role as a link in the hydrologic cycle (Benton *et al.*, 1950; Benton and Estoque, 1954; Starr and Peixoto, 1958), and its relation to the heat and water budget of the land or ocean surface (Möller and de Bary, 1951; Möller, 1951, 1952; Benton and Estoque, 1954; Nyberg, 1958; Colón, 1960; Väisänen, 1962). The present paper presents an analysis of the water vapor flux over the Central American seas as part of a more comprehensive study concerned with the general circulation and energetics in the Caribbean and Gulf of Mexico areas.

2. Methods of computation

The study is based on all available radiosonde ascents of 1960. Twice daily soundings at 0000 and 1200 GCT were at disposal for a total of 27 stations in the area of the Central American seas, as shown in Fig. 1. Two selected networks of ten stations for the Caribbean and the Gulf of Mexico areas, respectively, were used for the various divergence computations. Data for these 20 stations were in general complete. Greater gaps did exist for some of the stations not belonging to the above-mentioned divergence networks. Soundings at 0000 and 1200 GCT are combined in this representation; the topic of diurnal fluctuations will be dealt with elsewhere. Constant pressure levels of 1000, 950, 900, 850, 800, 750, 700, 600, 500, 400 and 300 mb were used in the analysis.

The water vapor flux in a certain level is given by

$$w=\rho_w \mathbf{V}=q\rho\mathbf{V}, \tag{1}$$

where ρ is density of the air, ρ_w water vapor density, q specific humidity, and $\mathbf{V}$ the wind vector. The resulting dimensions are (gm H_2O) cm^{-2} sec^{-1}. The water vapor transfer in a given level can also be written as

$$\tilde{w}=-\frac{1}{g}q\mathbf{V}, \tag{2}$$

where g is the acceleration of gravity, and the resulting units are (gm H_2O) (cm mb sec)$^{-1}$. The monthly mean

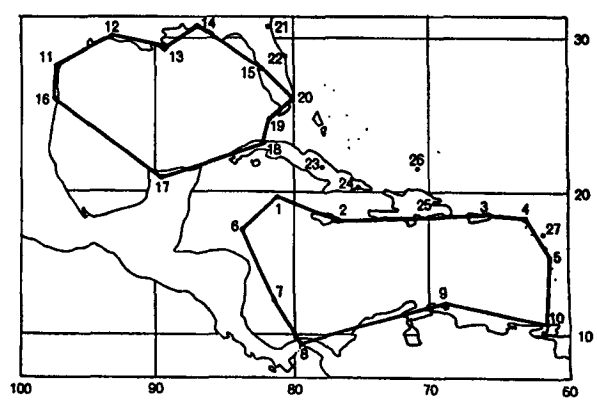

FIG. 1. Orientation map of stations used.

of the water vapor flux is approximated by the arithmetic mean of the fluxes computed for the individual soundings.

The water vapor transport in the entire atmospheric column is obtained by a vertical integration from the surface to the top of the water vapor atmosphere, i.e.,

$$W=\int_{\text{sfc}}^{300\text{ mb}} q\mathbf{V}\frac{dp}{g}. \tag{3}$$

In practice, the vertical integration is approximated by the trapezoidal rule, i.e., assuming a linear variation of the flux with height between adjacent pressure levels. It will be noticed that a fairly close spacing was chosen between the constant pressure levels used in the analysis.

The monthly mean of the water vapor transfer in a given level can be written as

$$\frac{1}{g}\overline{(q\cdot\mathbf{V})}=\frac{1}{g}[(\bar{q}\cdot\bar{\mathbf{V}})+\overline{(q'\cdot\mathbf{V}')}], \tag{4}$$

where the total transfer $(1/g)\overline{(q\cdot\mathbf{V})}$ is made up of two terms. The mean term $(1/g)(\bar{q}\cdot\bar{\mathbf{V}})$ can obviously be computed from the monthly mean of specific humidity and the resultant wind. The difference between the total flux $(1/g)\overline{(q\cdot\mathbf{V})}$ and the mean flux $(1/g)(\bar{q}\cdot\bar{\mathbf{V}})$, the term $(1/g)\overline{(q'\cdot\mathbf{V}')}$, represents the effect of pure time eddies and space-time eddies (correlation between specific humidity and wind vector, travelling disturbances). It does not include standing eddies. The eddy moisture flux is climatologically significant, and its pattern will be discussed in Section 4.

The horizontal divergence of the moisture flux in the entire atmospheric column is given by

$$\nabla\cdot W=\int_{\text{sfc}}^{300\text{ mb}}\nabla\cdot q\mathbf{V}\frac{dp}{g}=\int_{\text{sfc}}^{300\text{ mb}}(\oint qv_n dl)\frac{dp}{g}, \tag{5}$$

where v_n is the wind component normal to the element of perimeter dl. The divergence $\nabla\cdot q\mathbf{V}$ was evaluated separately for each of the constant-pressure levels used. Two different computational procedures were developed. In the first method, the u and v components of the flux are assumed to vary linearly in both the x and y directions. Coefficients for the u and v components of the flux at each of the 10 stations were calculated, on the basis of the method of least squares. The convergence of meridians poleward is taken into account in the determination of these coefficients. With this procedure, use can be made of stations located in the interior, not necessarily around the perimeter of an area. It is impractical to give greater details here.

The second method assumes that the u and v components of the flux vary linearly between adjacent stations around the perimeter. This is the assumption commonly implied in the line-integral procedure. Again, coefficients for the u and v components of the flux are calculated as constants for all of the 10 stations.

The two procedures give slightly different values and only the results of the second method are reported here. The propagation of instrumental and sampling errors and their influence on the final results were examined. It was found that the analysis on the basis of the available material and the combination into month-to-month averages are, in general, feasible. More serious limitations may occasionally be implied in the assumption of a linear variation of the fluxes in the x and y directions, or between adjacent stations around the perimeter, respectively.

3. The pattern of the total moisture flux

In tropical latitudes, the variation of radiation and temperature throughout the year is comparatively small, and the march of the seasons is reflected rather in the change of dry and rainy seasons. Hence, the flux pattern of the atmospheric water vapor is of particular interest for the understanding of seasonality and regional climatic characteristics. The water vapor flux pattern in the area of the Central American seas displays a pronounced variation throughout the year. Figs. 2 and 3 give a first orientation on the contrasting patterns between the winter and the summer half-years. On the basis of the characteristics of the atmospheric circulation, November through April are here counted as the winter half-year, and May through October as the summer. The water vapor flux pattern is, however, far from uniform for all months with either a winter or summer type circulation. Charts or cross sections of the moisture flux (Figs. 4–11) are reproduced here only for two characteristic months of each half-year.

Winter. The water vapor flux pattern in the winter half-year (Fig. 2) shows an essentially westward directed transport south of the 20N latitude circle. This westward total transfer of water vapor is concentrated in a relatively narrow band over the southern

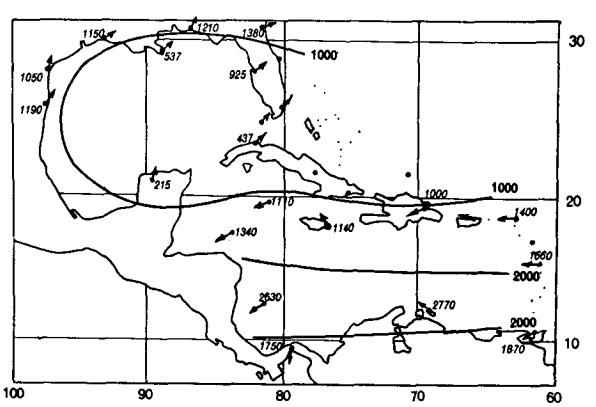

FIG. 2. Vertically integrated total flux of water vapor, November-April, in (gm H_2O) cm^{-1} sec^{-1}.

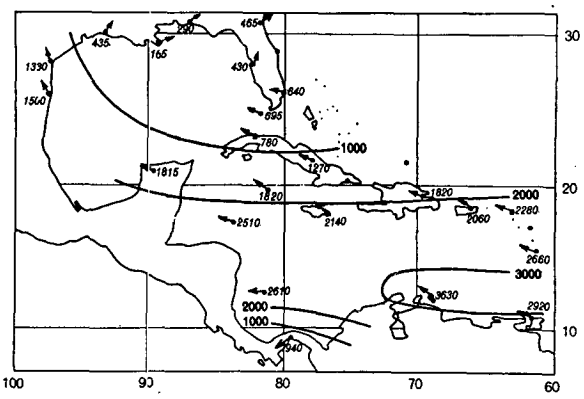

FIG. 3. Vertically integrated total flux of water vapor, May-October, in (gm H_2O) cm^{-1} sec^{-1}.

Caribbean Sea. It is characteristic that the transport clearly increases downstream. North of this zone with an essentially westward transfer, in a tongue extending approximately from Hispaniola over Cuba to Yucatan and southern Florida, a conspicuous change is apparent—the total vertically integrated water vapor transfer decreases drastically, and its direction changes gradually towards NW, N and then NE. Adjacent to this area, towards the NW over the Gulf of Mexico, a fairly strong flux prevails, directed roughly towards the NE. Over the Gulf of Mexico the transport is also obviously reinforced downstream. The tongue-shaped area, characterized by a minimum of the total water vapor transfer together with a strong directional variation, is clearly controlled by the latitude position and westward extension of the high pressure axis in the lower troposphere.

The vertical structure of the moisture flux can best be understood from meridional and zonal cross sections. Transects for only one month of each half-year were included in Figs. 5, 6, 9 and 10. Fig. 5 illustrates the vertical structure of the moisture flux in a meridional cross section along approximately 80W for January 1960. This gives an idea of the winter conditions.

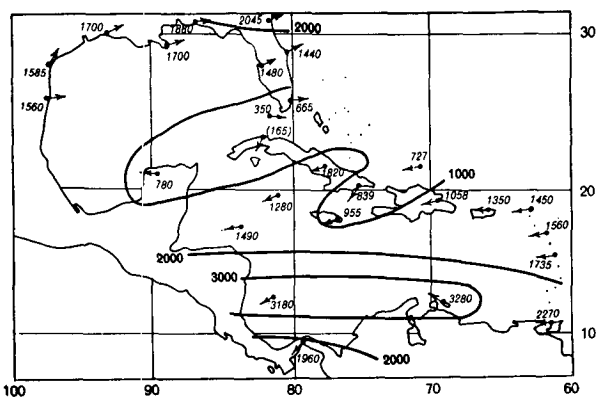

FIG. 4. Vertically integrated total flux of water vapor, January, in (gm H_2O) cm^{-1} sec^{-1}.

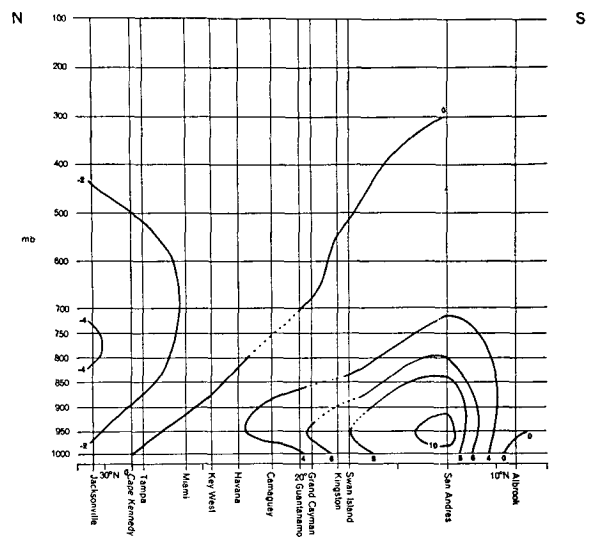

FIG. 5. Total zonal transport of water vapor in a cross section along approximately 80W, January, in (gm H_2O) (cm mb sec)$^{-1}$.

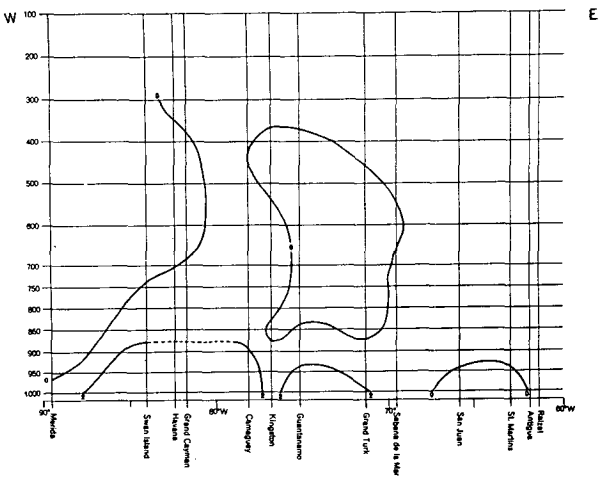

FIG. 6. Total meridional transport of water vapor in a cross section along approximately 20N, January, in (gm H_2O) (cm mb sec)$^{-1}$.

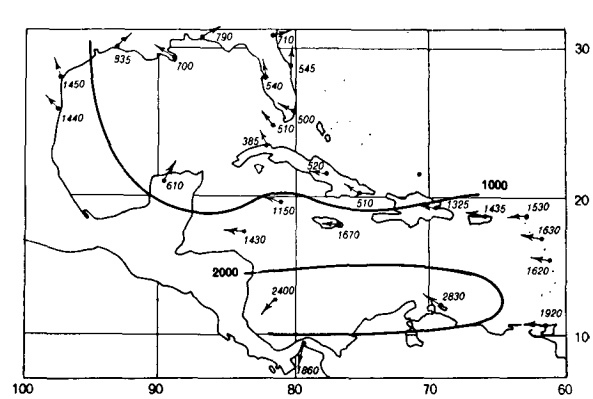

FIG. 7. Vertically integrated total flux of water vapor, April, in (gm H_2O) cm^{-1} sec^{-1}.

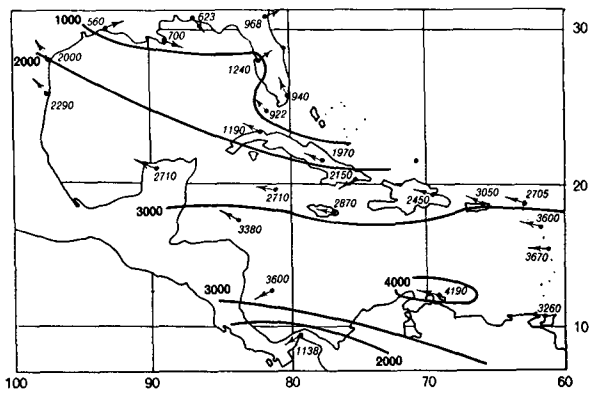

FIG. 8. Vertically integrated total flux of water vapor, July, in (gm H_2O) cm^{-1} sec^{-1}.

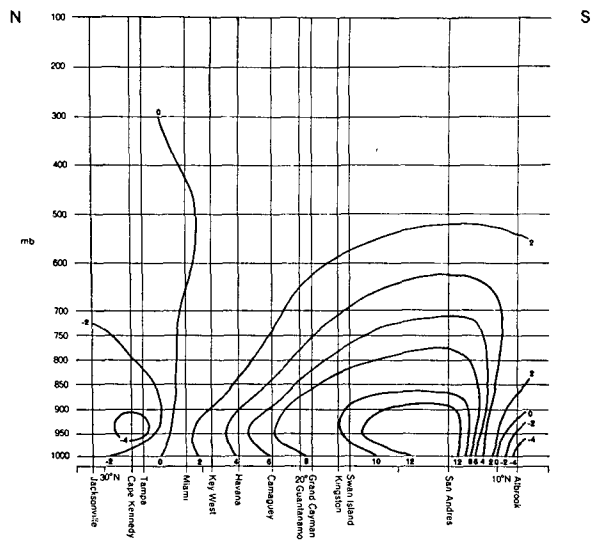

FIG. 9. Total zonal transport of water vapor in a cross section along approximately 80W, July, in (gm H_2O) (cm mb sec)$^{-1}$.

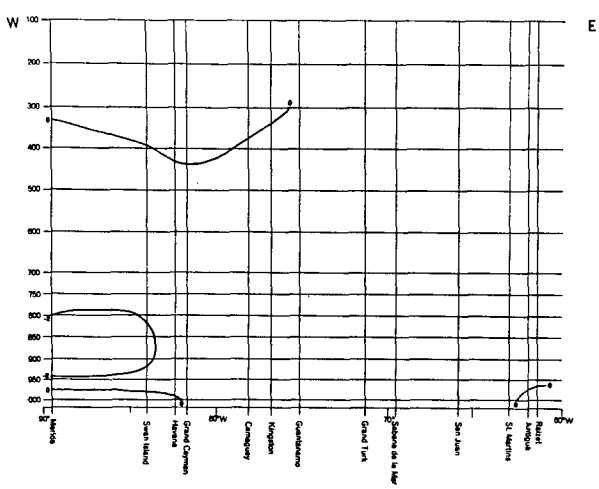

FIG. 10. Total meridional transport of water vapor in a cross secetion along approximately 20N, July, in (gm H_2O) (cm mb sec)$^{-1}$.

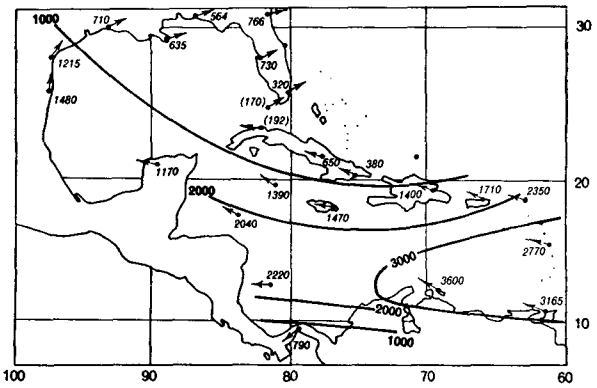

FIG. 11. Vertically integrated total flux of water vapor, October, in (gm H_2O) cm^{-1} sec^{-1}.

The westward directed transport has its maximum below the 900-mb level, and its core is clearly situated over the southern Caribbean Sea. A very shallow eastward transport is maintained throughout the year in the Panama area. In the lower layers, a weak westward transport is found as far north as southern Florida, at the beginning and again towards the end of the winter half-year. In any case, it is topped by a pronounced opposite transfer in higher layers. As to the meridional transports across the 20N transect (see Fig. 6), the direction is predominantly southward. This is in agreement with the large-scale wind pattern in the lower troposphere. The water vapor flux pattern displays marked variations in the course of the winter half-year, but they cannot be discussed here. The chart of the moisture flux pattern in April (Fig. 7) illustrates a development towards the summer conditions.

Summer. The water vapor flux pattern during the summer half-year as a whole is represented in Fig. 3. During the summer half-year, the area with minimal water vapor transfer is situated far north, this being associated with the seasonal displacement of the high pressure axis in the lower layers. A strong westward directed transport dominates in a broad band over the Caribbean Sea. The meridional transect along 80W for July (Fig. 9) illustrates the broad meridional and high vertical extension of the core of the moisture flow although there are conspicuous differences between the various months of the rainy season. A powerful moisture flow extends from the Caribbean and Caymán Seas over the western part of the Gulf of Mexico into the interior of the North American continent. A northward transport across the 20N latitude circle, as shown in the July transect (Fig. 10) is typical for the summer half-year. In contrast to the winter half-year the moisture transport during the rainy season tends to decrease downstream. The moisture flux pattern varies from one month to another, as do the atmospheric circulation and the weather characteristics in the course of the rainy season. Only a few characteristic features can be mentioned here.

A pronounced change in the water vapor flux pattern appears from May to June. The moisture flow from the Caymán Sea over the southwestern Gulf of Mexico northwestward into the interior of the North American continent is intensified. This moisture tongue reaches its strongest development in mid-summer and is vital for the precipitation conditions in the American Southwest (e.g., Bryson and Lowry, 1955).

The moisture flux pattern changes fairly markedly from June to July. This appears to be associated with the "mid-summer high jump" (Bryson and Lahey, 1958), a large-scale adjustment process in the hemispheric circulation. In July and August, the moisture flux over the Caribbean Sea reaches its strongest development, and it is most intense in the western part (see Fig. 8).

September and October show a moisture flux pattern definitely different from July and August (see Figs. 8 and 11). Atmospheric circulation and weather character in the Caribbean and Central American area during the late part of the rainy season are also known to contrast with the preceding months. The area of minimal moisture transport shifts gradually southward during September and October, associated with the seasonal displacement of the high pressure axis in the lower layers.

The eastward directed moisture transport begins to be concentrated over the southern Caribbean Sea, and there appears a tendency for a reinforcement of the flux downstream (see Fig. 11). A very conspicuous change is that the vigorous moisture flow extending from the Caymán Sea towards the southwestern United States in the previous summer months completely disappears in September. This change appears to be responsible for the end of the summer rains in the American Southwest. In the Gulf area, the moisture flux is still relatively weak, as compared to the winter season, but it has already acquired a dominant component eastward.

4. The eddy transfer

The characteristic features of the eddy flux will be reviewed in this Section. These transports are associated with time and space-time eddies, and they display significant seasonal and regional variations.

Winter. In the area of the Caribbean and Caymán Seas, the eddy flux of moisture is relatively small and its direction is somewhat irregular. In contrast, the eddy transport over the Gulf of Mexico in winter amounts to some 30–50 per cent of the total flux! The pattern given in Fig. 12 for January is representative of the winter conditions. The impressive eddy transfer over the Gulf of Mexico in winter reflects the strong horizontal, predominantly meridionally oriented, gradient of specific humidity from the northern fringe of the topical seas towards the cold interior of the North American continent. The strong meridional variation of the precipitable water is represented in Fig. 13 for January. In the tropics proper, on the other hand, over the Caribbean Sea, the horizontal distribution of atmospheric humidity is, by and large, much more uniform, the directional steadiness of the trade winds being well known. This accounts for the much weaker and rather irregular eddy flux in the area of the Caribbean and Caymán Seas. Even there, however, the eddy flux appears largely to follow the horizontal gradient of the moisture field

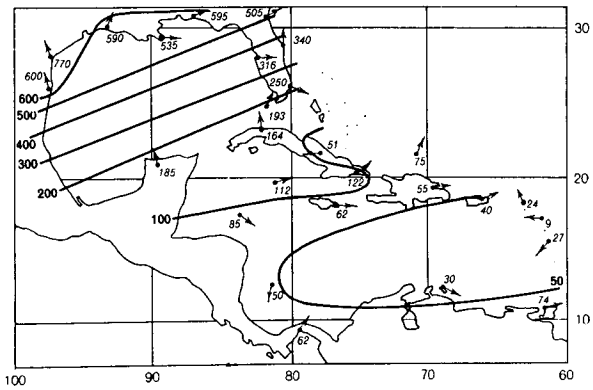

FIG. 12. Vertically integrated eddy flux of water vapor, January, in (gm H_2O) cm^{-1} sec^{-1}.

The eddy flux in the Gulf area increases strongly from the end of the rainy season towards mid-winter. This is associated with the increasing meridional contrasts in the atmospheric moisture field. The eddy moisture flux over the Caribbean remains comparatively small. The northward directed eddy moisture flux in the Gulf area becomes strongest in January and February.

The transition towards the summer pattern in April also becomes apparent in the decreased eddy flux in the Gulf area. The dominating large-scale meridional gradient in the moisture field from the tropical seas to the interior of the North American continent, so characteristic for the winter season, weakens gradually.

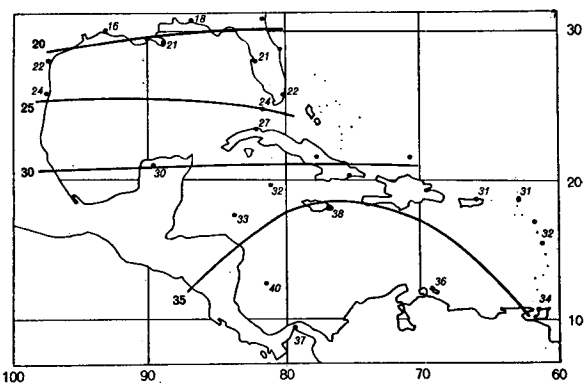

FIG. 13. Distribution of precipitable water, January, in mm H_2O.

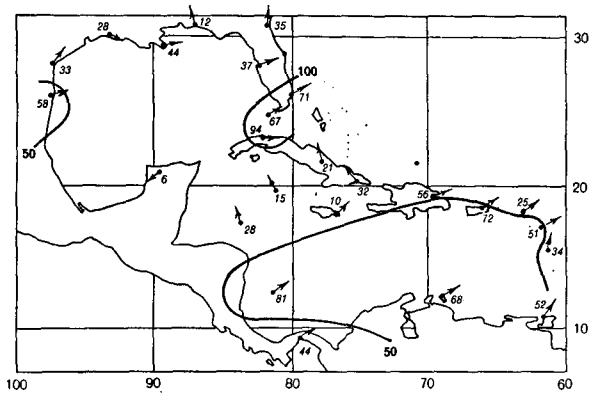

FIG. 14. Vertically integrated eddy flux of water vapor, July, in (gm H_2O) cm^{-1} sec^{-1}.

Summer. During the summer half-year, the eddy moisture fluxes over the Gulf of Mexico are about as small and irregular as over the Caribbean Sea (see Fig. 14) and the field of specific humidity is horizontally rather uniform all over the Central American seas (see Fig. 15).

During May and June, the eddy flux in the Gulf area appears diminished in comparison with the previous months; however, it still amounts to some 20 per cent or more of the total flux and is directed rather uniformly northward into the interior of the North American continent. In July and August, the eddy fluxes become small and rather irregular in their direction over both the Gulf of Mexico and the Caribbean and Caymán Seas (see Fig. 14).

The broad-scale change of the circulation pattern in September is associated with a steepening of the horizontal gradients in the field of specific humidity. This is also reflected in the field of the eddy flux of water vapor. The eddy flux in the Gulf area grows stronger and is essentially directed northward.

In October, the eddy flux is further increased in the Gulf area, contributing now some 30 or occasionally even more than 50 per cent to the total flux and its direction is generally northward. The eddy fluxes over the Caribbean Sea continue to be rather weak and irregular.

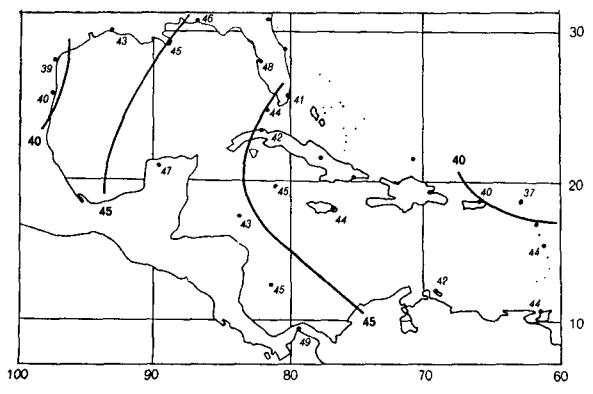

FIG. 15. Distribution of precipitable water, July, in mm H_2O.

5. The divergence of the water vapor flux

The budget equation of atmospheric water vapor in a column extending from the surface to the top of the water vapor atmosphere can be written as

$$(E-P)=\int_{\text{sfc}}^{300\text{ mb}}\frac{\partial q}{\partial t}\frac{dp}{g}+\int_{\text{sfc}}^{300\text{ mb}}\nabla\cdot q\mathbf{V}\frac{dp}{g}+(\overline{\rho q\cdot w})_{300\text{ mb}}. \tag{6}$$

Here E means large-scale evaporation from the ocean surface and P large-scale precipitation in the area considered.

The limitations of this formulation have recently been discussed by Schmitz (1963) in a critical review of the problem. The net import or export of water vapor by clouds moving through the area, as well as the storage of water in droplet form, are disregarded in the above formulation. This appears justified, if larger areas and sufficiently long periods of time are considered.

Concerning the third right-hand term in Eq. (6), it would, in practice, only be feasible to compute the transport by the mean vertical motion, on the basis of the time-area means of the vertical velocity w, and the specific humidity q, respectively. While the eddy component could not be assessed directly, the vertical transport through the top of the atmospheric column can, in general, be disregarded, if the vertical integration is extended to a sufficiently high level, where the water vapor content becomes small. A comparison of the order of magnitude of the different terms in Eq. (6) indicates that 300 mb can be considered as a sufficiently high level.

The storage of water vapor within the atmospheric column, $\int(\partial q/\partial t)(dp/g)$, can be computed from radio soundings at the beginning and the end of the time period considered. The time rate of change of the water vapor content of the atmospheric column becomes comparatively small, if greater periods of time, say a month, are considered. With thse reservations, the vertically integrated water vapor flux divergence is found to be equal to the difference of large-scale evaporation minus precipitation, i.e.,

$$(E-P)=\int_{\text{sfc}}^{300\text{ mb}}\nabla\cdot q\mathbf{V}\frac{dp}{g}. \tag{7}$$

Then, the water vapor added to the atmospheric column by evaporation at the sea-air interface must meet the loss of water by precipitation within the area considered and by the lateral export of water vapor, that is, the vertically integrated water vapor flux divergence. A qualitative idea of the divergence of the water vapor flux has already been given in the discussion of the moisture flux pattern in the various seasons of the year. During the winter half-year, the moisture flux tends to increase downstream, over both

the Caribbean Sea and the Gulf of Mexico. This represents a divergence of the water vapor flux, i.e., a net export from the area considered. This agrees with the concept of the trades as exporters of latent heat. During the greater part of the summer half-year, the moisture flux over the Caribbean Sea was found to decrease downstream, except in July and August. Over the Gulf of Mexico, the moisture flux pattern indicates a tendency to convergence only in July and August. The implications of the latent heat flux for atmospheric energetics and general circulation in the area of the Central American Seas has been discussed in more detail elsewhere (Hastenrath, 1966).

A first qualitative idea of the divergence or convergence of the moisture flux can already be obtained from the charts of the water vapor flux pattern (Figs. 2, 3, 4, 7, 8, 11). For a quantitative assessment of the moisture flux divergence, the computational procedure described in Section 2 was applied. The lateral export or import of water vapor in finite atmospheric layers was computed for the Caribbean Sea and the Gulf of Mexico on a sounding-to-sounding basis, and it was then combined into monthly averages. The station networks used for the Caribbean and the Gulf areas are represented in Fig. 1. From the imports and exports in the various finite layers the divergence in the entire atmospheric column

$$\nabla \cdot W = \int \nabla \cdot q \mathbf{V} \frac{dp}{g},$$

was computed. The seasonal march of the vertically integrated water vapor flux divergence is represented in Fig. 16 for the Caribbean Sea and the Gulf of Mexico separately. The water vapor flux divergence in the entire atmospheric column is expressed in mm H_2O $(day)^{-1}$.

In the area of the Caribbean Sea the export of water vapor is largest from January through March. With the beginning of the rainy season a net import of water vapor begins to develop. July and August, which are known to have a weather character different from the other months of the rainy season, show a change to a slight divergence of the water vapor flux. There is again a convergence of the moisture flux in September and October.

The troposphere over the Gulf of Mexico exports water vapor during the greater part of the year. A convergence of the moisture flux does, however, develop in summer, reaching its peak in August. A convergence of the moisture flux was also calculated for April 1960. This, however, appears, to have been a somewhat abnormal month since abnormally high precipitation was reported in the Gulf States (O'Connor, 1960; U. S. Weather Bureau, 1960), a conspicuous upward motion was computed from the aerological data, and the trade inversion was less frequent than in the adjacent months (Hastenrath, 1966). It must also be mentioned that the results of the divergence computations for September are probably biased towards too high values. A lower- and mid-tropospheric trough appears to be located over the Florida Straits and southern Florida, in agreement with the climatic mean conditions stated by Riehl (1947). The westward extension of this trough cannot be traced with the available data. This means that the import of water vapor in the southwestern part of the Gulf of Mexico is probably greater than the values resulting from the assumptions made for the present computations.

The water vapor flux divergence is found to be equal to the difference between large-scale evaporation and precipitation. The relation of moisture flux divergence, evaporation from the sea surface and precipitation, will be discussed in the following section.

6. The annual march of precipitation, evaporation, and water vapor flux divergence

The water vapor flux pattern and its seasonal variations play an important role in precipitation, particularly where local or regional topography provides for convergence and ascending motion.

Over the Caribbean Sea, a pronounced westward transfer of moisture also takes place in the winter half-year, the flux being rather from the NE over the Caymán Sea and the western part of the Caribbean Sea and Central America. This provides for abundant precipitation on the windward side of the mountainous islands, along the high mountain ranges of Central America and along the coastlines (Bryson and Kuhn, 1961; Hastenrath, 1967) where convergence and ascending motion of a more local or small regional scale play an important role. Local contrasts in the precipitation distribution can be particularly sharp at this time of year.

In the Gulf area in summer, a strong moisture flux is directed around the western tip of the high pressure cell into the Gulf States and toward the interior of the North American continent. The moisture flux pattern over the southern United States in 1960 agrees closely with that found by Benton and Estoque (1954) for the year 1949. The rainfall regime in the Gulf States, the Southern Plains and above all the American Southwest, with its pronounced summer peak [see also Bryson and Lowry (1955)], is largely controlled by the moisture supply from the Gulf of Mexico, and the seasonal variations of the water vapor flux pattern.

The role of the moisture flux pattern for the march of precipitation in the land areas around the Central American seas is particularly apparent where the local topographic conditions are favorable. A far more dominating control of the large-scale rainfall regime is found, however, in the season variations of the field of vertical motion.

The large-scale vertical motion in each month was calculated by the kinematic method, for the areas

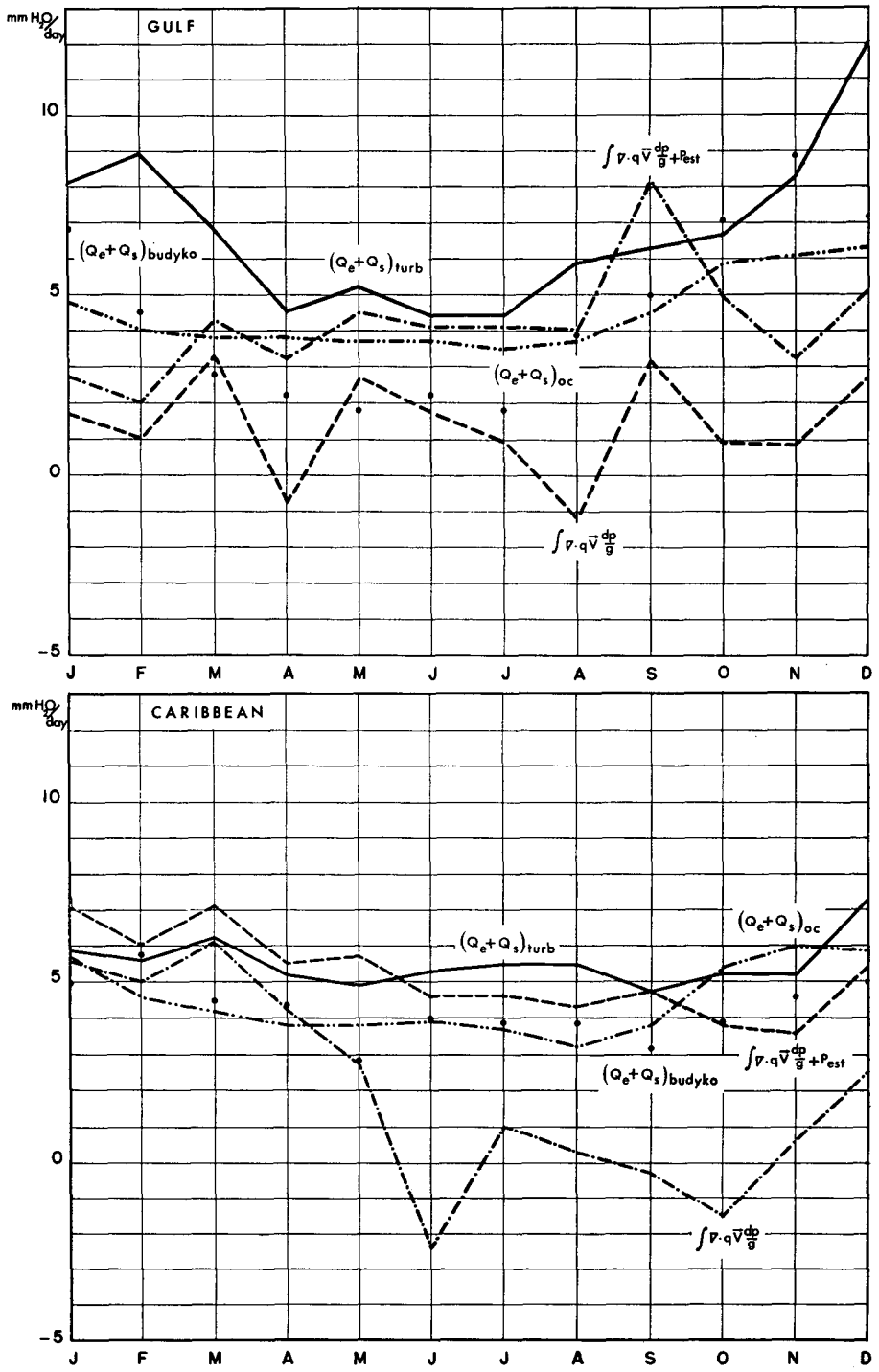

FIG. 16. Seasonal march of the vertically-integrated water vapor flux divergence, $\int_{sfc}^{300} \nabla\cdot q\mathbf{V}\frac{dp}{g}$; the sum of vertically integrated water vapor flux divergence and large-scale precipitation estimated from island and coastal stations, $\left(\int_{sfc}^{300} \nabla\cdot q\mathbf{V}\frac{dp}{g}+P_{est}\right)$; the sensible and latent heat flux at the sea-air interface as computed by the bulk-aerodynamic method from 1960 ship observations, $(Q_s+Q_e)_{turb}$; and the sensible and latent heat flux at the sea-air interface as estimated from the quasi multi-annual oceanic budget, $(Q_s+Q_e)_{oc}$.

of the Gulf of Mexico and the Caribbean Sea separately. For the computations of the horizontal wind divergence a procedure corresponding to that described in Section 2 was applied. Networks of ten stations each were used in the two areas, as represented in Fig. 1. Vertical velocities were computed for the 850-, 700-, 500- and 300-mb levels. The annual march of vertical motion at the 700-mb level is shown in Fig. 17.

Independently, the mean vertical motion in the layer from the surface to 300 mb was computed by the thermodynamic method. Results are in fair agreement with those of the kinematic method. Seasonal variations in the field of vertical motion are particularly pronounced over the Caribbean Sea. A detailed analysis of the standard pressure levels shows that the seasonal and regional characteristics in the field of vertical motion are associated with variations in strength and position of the western tip of the North Atlantic anticyclone. Discussion of greater details appears inappropriate here.

The large-scale vertical motion over the Caribbean Sea is upward, up to the 300-mb level, throughout a great part of the year. The maximum values appear in June and in September and October, while the mean ascending motion is clearly weaker during July and August. Downward motion is indicated in the lower and mid troposphere from January to May, with the strongest subsidence clearly in March. Over the Gulf of Mexico, descending motion is found through most of the year, with the strongest subsidence apparently around February and March. Upward motion develops, however, especially in July and August.

The annual march of precipitation in 1960 in the Caribbean and the Gulf of Mexico areas, as estimated from island and coastal stations, can be obtained from Fig. 16. The rainfall regime in the area of the Caribbean Sea appears to be controlled predominantly by the field of large-scale vertical motion. Both ascending motion and rainfall amounts, roughly increase from late spring to late fall. Late winter and early spring, when a pronounced downward motion develops over the Caribbean Sea, are the periods of most pronounced drought. The agreement is striking when individual months are analyzed.

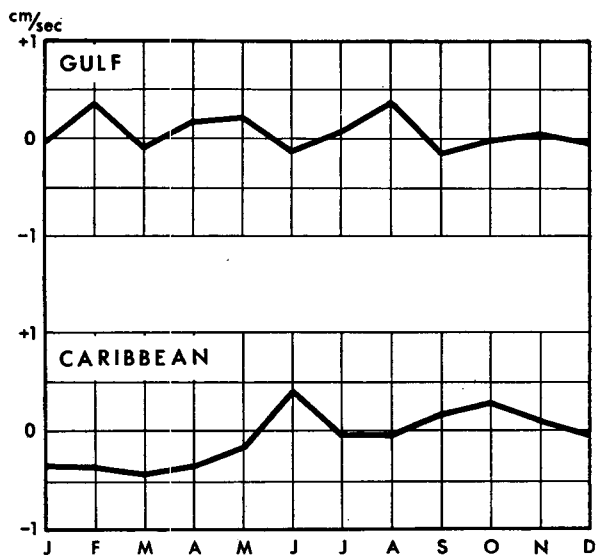

FIG. 17. Seasonal march of large-scale vertical motion at the 700-mb level over the Caribbean Sea and the Gulf of Mexico.

On the Central American Isthmus with its complex orography, a large variety of rainfall distribution and regime is found, which would be inappropriate to discuss in greater detail here.

Lahey (1958) found his results inconclusive for explaining the late winter dryness over the Netherlands Antilles. This now appears understandable since Lahey combined the three months of each season in his computations of vertical velocity in order to account for the quality of the available material.

A rough qualitative agreement between vertical motion and rainfall regime is also found in the area of the Gulf of Mexico, where the maxima of precipitation amounts and large-scale ascending motion coincide in summer.

A rather peculiar feature of the rainfall regime is the secondary minimum in July and August, which is indicated in large parts of the area of the Caribbean Sea, in Central America, and in at least the southern part of the Gulf of Mexico.

A double peak in the annual march of precipitation is known for large parts of the tropics (e.g., Haurwitz and Austin, 1944; Riehl, 1954), and it is traditionally explained by the double passage of the equatorial trough (Riehl, 1954). This may, in fact, hold true for large areas, but with regard to the American sector, however, the equatorial trough apparently barely ever reaches the southern margin of the Caribbean Sea, let alone a hypothetical double passage. Riehl (1947, 1954) suggested that the low-latitude portion of a polar trough and its seasonal shift might be responsible for the double summer peak of rainfall in parts of the Gulf area.

It appears that three factors above all have to be considered for the understanding of the double peak in the annual march of precipitation in the area of the Central American Seas. These are: 1) the large-scale ascending motion over the Caribbean Sea decreases during July and August in association with the westward extension of the North Atlantic high pressure cell; 2) sudden and extended dry spells (canículas in Central America) typically occur in July and August which, according to synoptic-climatological experience in Central America, are associated with a northerly flow in the upper troposphere. Similar conditions are indicated for the area of the Caribbean Sea [compare Lahey (1958)]; 3) for the Eastern Pacific off the coasts of Central America and northern South America, a seasonal variation in the latitude position of the ITC is reported, with a slight southward shift during July

and August (Alpert, 1945, 1946 a, b). There are indications that "temporales" develop from disturbances in the ITC which account for abundant rainfall above all on the Pacific side of Central America, most commonly during June, September and October.

The annual march of precipitation appears to be determined above all by the field of large-scale vertical motion, apart from regional topographic effects and certain other processes. The annual march of precipitation in the area of the Caribbean Sea in a large-scale picture shows a minimum around February and March, a sharp and steady increase towards summer, the main rainy season, a secondary minimum around July and August, and, after the second peak around September and October, a steady decrease towards winter. Precipitation in the Gulf area increases from a minimum around February to a marked peak around August and September, and then drops steadily towards late winter. This is, of course, only a generalized picture and regional differences do exist.

The annual variation of evaporation closely follows the march of the temperature difference at the sea-air interface (see Figs. 16 and 18). This implies a maximum in fall and a decrease towards summer. Phase differences are found for the two sea areas, reflecting the geographic latitude. Estimates of the sensible and latent heat flux at the sea-air interface by various independent methods are reviewed in Section 7. The annual variation of evaporation is relatively small as compared to the march of precipitation.

The seasonal march of the water vapor flux divergence obviously results from the variation of both evaporation and precipitation. Qualitatively, this means for the area of the Caribbean Sea a maximum around March,

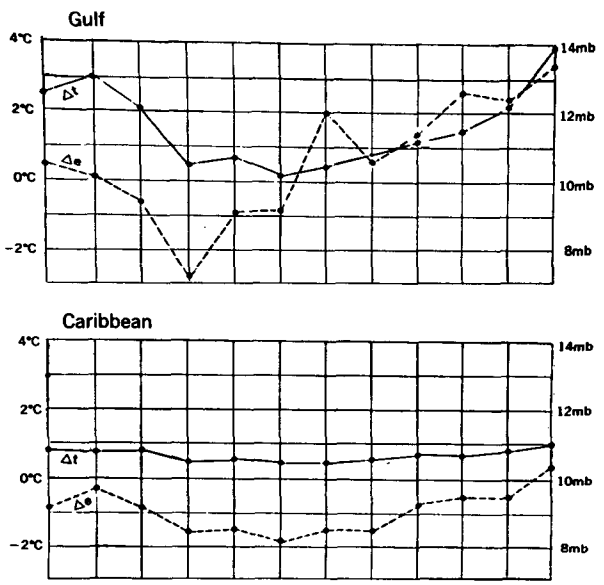

FIG. 18. Seasonal march of the temperature difference Δt, and the water vapor difference Δe, at the sea-air interface (1960 ship observations).

and a marked decrease with the onset of the rainy season, from about May onward. A secondary maximum then appears around July and August, together with the midsummer minimum in rainfall. The water vapor flux divergence reaches a second minimum around October, after which there is a steady increase towards early spring, with the associated decrease in rainfall activity.

In the discussion of the water vapor flux divergence in the Gulf area (Section 5), it was pointed out that April 1960 represents an abnormal month, and that the computations for September are probably biased. Apart from this, the water vapor flux divergence seems to have relatively high values in late winter and spring, dropping to a minimum in late summer and early fall (see Fig. 16).

In addition to this rather qualitative discussion of the annual march, a quantitative comparison of the water vapor flux divergence with independent estimates of the large-scale precipitation and the evaporation from the sea surface is of interest. A review of this problem is included in the following section.

7. The latent and sensible heat flux at the sea-air interface

With certain restrictions mentioned above, the water vapor flux divergence can be considered as equal to the difference of large-scale evaporation and precipitation. Within certain limits of accuracy, it is also possible to obtain the sum of the sensible heat flux from the surface and the precipitation heating inside the atmospheric column ($LP+Q_s$), as a residual in the atmospheric energy budget. This amounts to an estimate of the latent and sensible heat flux from the sea suface (Q_e+Q_s), from the atmospheric moisture and energy budgets alone, on the basis of aerological data.

Independently, the latent and sensible heat flux at the sea-air interface can be computed by the bulk aerodynamic method, on the basis of such ship observations as sea surface temperature, wind speed, temperature and humidity at deck level. Malkus (1962) derived formulae for the evaporation

$$E=0.092(e_w-e_a)v \tag{8}$$

and the corresponding sensible heat flux

$$Q=0.059(t_w-t_a)v. \tag{9}$$

Here the sea surface temperature t_w and the air temperature t_a are in °C, the vapor pressure e_a of the air at the level where temperature and wind is measured and the saturation vapor pressure e_w belonging to the temperature of the sea surface are in mb, the wind speed v at ship's deck level is in m sec^{-1} and the evaporation E and the sensible heat flux Q are in equivalents of (mm H_2O) day^{-1}.

For the area of the Caribbean Sea some 2000–3000 ship observations per month were available for 1960,

with 3000–4000 for the area of the Gulf of Mexico using data obtained from the National Weather Records Center. The results of the computations on the basis of Malkus' formulae are included in Fig. 16. Furthermore, the latent and sensible heat flux at the sea-air interface can be calculated on a quasi multi-annual basis as a residual in the heat budget equation of the oceanic water body, by a procedure similar to that used by Colón (1960). The results of this computation are also included in Fig. 16, for the Caribbean Sea and the Gulf of Mexico separately.

In Fig. 16 evaporation estimates based on the atmospheric moisture budget and the observed precipitation for 1960 can be compared with the values of the the latent and sensible heat flux obtained from the oceanic heat budget, on a quasi multi-annual basis. Making allowance for the propagation of instrumental and sampling errors in the atmospheric budget, and inter-annual variations, the agreement appears satisfactory. The results of the bulk-aerodynamic method, on the basis of the 1960 ship observations, on the other hand, differ conspicuously from those of the two other methods, above all during the winter season. This appears to be due primarily to the inadequacy of ship observations.

The estimation of the latent and sensible heat flux in the area of the Central American seas by the various independent methods will be discussed in greater detail elsewhere. In view of the shortcomings inherent in any of these methods, it appears advisable to apply all independent approaches wherever feasible.

Acknowledgments. This study was supported by the National Science Foundation under Grant GP 444. Thanks are particularly due to Reid A. Bryson for his constructive criticism. Lois Suomi and Phil Schmidt did the programming for the CDC 1604 and IBM 1620 computers.

REFERENCES

Alpert, L., 1945: The intertropical convergence zone of the Eastern Pacific region, I. *Bull. Amer. Meteor. Soc.*, **26**, 426–432.

——, 1946a: The intertropical convergence zone of the Eastern Pacific region, II. *Bull. Amer. Meteor. Soc.*, **27**, 15–29.

——, 1946b: Weather over the tropical Eastern Pacific Ocean, 7 and 8 March 1943. *Bull. Amer. Meteor. Soc.*, **27**, 384–398.

Benton, G. S., R. T. Blackburn and V. O. Snead, 1950: The role of the atmosphere in the hydrologic cycle. *Trans. Amer. Geophys. Union*, **31**, 61–73.

——, and M. A. Estoque, 1954: Water vapor transfer over the North American continent. *J. Meteor.*, **11**, 462–477.

Bryson, R. A., and P. M. Kuhn, 1961: Stress-differential induced divergence with application to littoral precipitation. *Erdkunde*, **15**, 287–294.

——, and J. F. Lahey, 1958: The march of the seasons. Dept. Meteorology, Univ. Wisconsin, AFCRC-TR-58-223, Final Report Contract AF 19(604)-992, 41 pp. (ASTIA No. AD-152500).

——, and W. P. Lowry, 1955: Synoptic climatology of the Arizona summer precipitation singularity. *Bull. Amer. Meteor. Soc.*, **36**, 329–339.

Colón, J. A., 1960: On the heat budget of the troposphere and water body of the Caribbean Sea. National Hurricane Research Project, Report No. 41, U. S. Dept. Commerce, Washington, D. C., 65 pp.

Hastenrath, S., 1966: On general circulation and energy budget in the area of the Central American Seas. *J. Atmos. Sci.*, **23**, 694–712.

——, 1967: Rainfall distribution and regime in Central America. *Arch. Meteor., Geophys., Bioklimatol.*, Ser. B, in press.

Haurwitz, B., and J. M. Austin, 1944: *Climatology*. New York, McGraw-Hill, 410 pp.

Hutchings, J. W., 1957: Water vapor flux and flux-divergence over Southern England: summer 1954. *Quart. J. R. Meteor. Soc.*, **83**, 30–48.

Lahey, J. F., 1958: On the origin of the dry climate in northern South America and the southern Caribbean. Sci. Report No. 10, Dept. Meteorology, Univ. Wisconsin, AFCRC-TN-58-218 (ASTIA AD-146868), 290 pp.

Malkus, J. S., 1962: Large-scale interactions. *The Sea, Vol. I, Physical Oceanography*, New York, Interscience, 88–294.

Möller, F., 1951: Bestimmung der Landesverdunstung durch Grossaustausch. *Ann. Meteor.*, 4, 157–160.

——, 1952: Zur Bestimmung der Gebietsverdunstung aus der Advektion. *Ber. Deut. Wetterdienst., U. S. Zone*, **5**, No. 35, 172–174.

——, and E. de Bary 1951: Der Wärme—und Wasserdampfhaushalt der freien Atmosphäre. *Arch. Meteor., Geophys. Bioklimatol.*, Ser. A, No. 4, 142–155.

Nyberg, A., 1958: A determination of some monthly values of evapotranspiration in Finland and in a region in the northeastern Atlantic. *Geophysica*, **6**, 377–387.

O'Connor, J. F., 1960: The weather and circulation of April 1960. *Mon. Wea. Rev.*, **88**, 158–166.

Riehl, H. 1947: Subtropical flow patterns in summer. Dept. Meteorology, Univ. Chicago, Miscellaneous Reports 22, 64 pp.

——, 1954: *Tropical Meteorology*. New York, McGraw-Hill, 392 pp.

Schmitz, H. P., 1963: Zu den Beziehungen für den fluktuativen und mitteren Wasserdampftransport in der Atmosphäre. *Geofis. Pura Appl.*, **55**, 217–238.

Starr, V. P., and J. P. Peixoto, 1958: On the global balance of water vapor and the hydrology of deserts. *Tellus*, **10**, 188–194.

——, and ——, 1960: On the zonal flux of water vapor in the Northern Hemisphere. *Geofis. Pura Appl.*, **47**, 199–203.

——, and ——, 1964: The hemispheric eddy flux of water vapor and its implications for the mechanics of the general circulation. *Arch. Meteor., Geophys., Bioklimatol.*, Ser. A, **14**, 111–130.

——, —— and G. C. Livadas, 1958: On the meridional flux of water vapor in the Northern Hemisphere. *Geofis. Pura Appl.*, **39**, 174–185.

——, and R. M. White, 1955: Direct measurement of the hemispheric poleward flux of water vapor. *J. Marine Res.*, **14**, 217–225.

Sutcliffe, R. C., 1956: Water balance and the general circulation of the atmosphere. *Quart. J. R. Meteor. Soc.*, **82**, 385–396.

U. S. Weather Bureau,1960: Climatological data (Florida, Louisiana, Texas). Vol. 66, No. 4. Available from National Weather Records Center, Asheville, N. C.

Väisänen, A., 1962: A computation of the evaporation over Finland during a rainless period based on the divergence of the water vapor flux. *Geophysica*, **8**, 159–165.